

# Adsorption of Collagen Nanofibrils on Rough TiO<sub>2</sub>: A Molecular Dynamics Study\*\*

By Wenke Friedrichs, Bastian Ohler, Walter Langel, Susanna Monti  
and Susan Köppen\*

*Classical molecular dynamics simulations of tropocollagen molecules on rough titania surfaces are presented. On the basis of plane rutile (100), two models for surface roughness have been adopted: (1 × 3) microfacets with dimensions of less than 14 Å had only minor influence on the adsorption of a triple helical structure with a diameter of about 16 Å. After increasing the roughness by terraces, steric hindrance of helix binding was observed. A model for telopeptide capping of the collagen triple helices was developed. The highly flexible telopeptide structures mediated adsorption on the surface and inserted into grooves of both surface models. The telopeptide β-turn motifs at the C-terminus of the tropocollagen interact with specific receptor regions of the triple helices. This intermolecular process seems to be entropy driven and may be the first step of assembling helices to ordered fibrils. Interaction between telopeptide and triple helix seems to be in competition with the rather enthalpy controlled surface adsorption of single collagen molecules.*

An atomistic picture of the biointerface between titanium oxide surfaces and proteins of the extracellular matrix is essential for understanding the initial steps for incorporation of titanium-based medical implants into physiological tissues in detail. The physicochemical properties of the TiO<sub>x</sub>/collagen interface essentially determine the biocompatibility, and

specific protein coatings like collagen can dramatically enhance the growth of new bone tissue.<sup>[1,2]</sup>

Protein adsorption on aqueous titania<sup>[2–4]</sup> and material surfaces in general<sup>[5–7]</sup> has recently been investigated in several experiments. Real surfaces are usually rough and can be described by steps, terraces, and vacancies.<sup>[8,9]</sup> Surface roughness from the macroscopic down to nanometer scale can influence protein adsorption.<sup>[4–6]</sup> Whereas the amount of collagen adsorbed on polymer surfaces with roughness in the range from 5 to 40 Å was nearly constant, significant differences in the morphology of the adsorbate were observed.<sup>[6]</sup>

A number of theoretical investigations focused on the peptide surface interaction at an atomistic level,<sup>[10–15]</sup> and included adsorption of dipeptides,<sup>[10]</sup> and other small peptides<sup>[3,12,13]</sup> on rutile and of protein fragments on flat surface models.<sup>[14,15]</sup> Simulations revealed that the immobilization of these biomolecules was due to the direct interaction between charged amino acids and surface atoms. The possibility of peptide adsorption on the stoichiometric (110) rutile surface through the first water layer was reported<sup>[13]</sup> but the penetration of protein groups and replacement of adsorbed water molecules with protein atoms was also observed.<sup>[16]</sup> Indeed, the study of direct adsorption of charged protein side chains to oppositely charged surface groups<sup>[12,14]</sup> on the hydroxylated model of the (100) rutile surface<sup>[17]</sup> confirmed this view. The hydroxylation equilibria introduce charged surface groups and have essential influence on the

[\*] W. Friedrichs, B. Ohler, W. Langel, S. Köppen  
Institute for Biochemistry, University of Greifswald, Felix-  
Hausdorff-Strasse 4, 17487 Greifswald, (Germany)

S. Monti

Institute of Chemistry of Organometallic Compounds (IC-  
COM-CNR) Area della Ricerca, via Moruzzi 1, 56124 Pisa,  
(Italy)

S. Köppen

Hybrid Materials Interfaces Group, Faculty of Production  
Engineering and Bremen Center for Computational Materials  
Science, University of Bremen TAB-Building, Am Fallturm 1,  
28359 Bremen, (Germany)

E-mail: koeppen@hmi.uni-bremen.de

[\*\*] We gratefully acknowledge assistance of Ying Gao (Shanghai)  
for the atomistic rough surface model and Robert Wolf (Greifswald)  
for doing some of the simulations. We thank the DEISA  
Consortium ([www.deisa.eu](http://www.deisa.eu)), co-funded through the EU FP6  
project RI-031513, and the FP7 project RI-222919, for support  
within the DEISA Extreme Computing Initiative (Project  
Acronym: TiO2COL) and COST D41 and the "Deutsche  
Forschungsgemeinschaft" (DFG) for financial support.

amino acid adsorption.<sup>[11]</sup> As described in ref.,<sup>[14]</sup> stable adsorption can be obtained even when the number of contacts is small, in fact the investigated 80 Å collagen fragments were attached to the surface by only two to three lysine or glutamic acid contacts and the major part of the flexible triple helix was floating in solution. Longer collagen helices will show enhanced flexibility, which may favor self-assembly.<sup>[18,19]</sup> Surface adhesion can only compete with it and result in stable adsorption if a large number of contacts is formed constraining thermal and hydrodynamic motion of the large molecule.

The RGD sequence, which typically mediates interactions between collagens or fibronectin and cells, is also part of titanium binding peptide motifs like TBP1.<sup>[20]</sup> At physiological pH values, the side chains of ARG and ASP in this sequence are positively and negatively charged resulting in a highly polar contact. Classical molecular dynamics simulations of an RGD peptide on a rectangular grooved surface revealed that the adsorption of a peptide is more stable on rough than on flat surfaces.<sup>[21]</sup> In an implicit water environment, aspartic acid was directly attached to fivefold coordinated surface titanium atoms on the edge of the ridges.

The elastic properties of collagen are of fundamental interest for specific characteristics of various biological tissues and have been studied exhaustively<sup>[22]</sup> both in experiment<sup>[23]</sup> and theory.<sup>[24–26]</sup> When collagen fibrils are stretched, inter- and intramolecular interactions generate stress response. For individual collagen triple helical molecules, forces of the order of a few pN are found at end to end distances below the molecule contour length, according to the Marko–Siggia equation for the wormlike chain model.<sup>[23]</sup> Experimental Young's moduli of collagen molecules were measured under strain by electron microscopy (3.0–5.1 GPa<sup>[27]</sup>), by X-ray diffraction (2.8–3.0 GPa<sup>[28]</sup>), and by optical tweezers (0.35–12.2 GPa<sup>[23]</sup>).

In the limit of small strain (10–20%), steered molecular dynamics simulations using GROMACS and CHARMM resulted in Young's moduli of 2.51–4.59 GPa<sup>[26]</sup> and about 10 GPa,<sup>[25]</sup> respectively, whereas a calculation of energy versus length using the force field AMBER3 yielded 1.33–2.41 GPa.<sup>[29]</sup> Buehler<sup>[25]</sup> reported significant stiffening at strain above 0.35 with a Young's module of up to 46.7 GPa, and attributed this effect to linear stretch of covalent bonds. Deviations between different simulations for comparable strain suggest that calculated Young's moduli are force field dependent, and that any atomistic model of the mechanical properties of collagen has to be validated. Force field parameters are optimized on the basis of short range interactions, and may not reproduce macroscopic mechanical properties equally well.

The triple helical region of the collagen type I molecules consists of two  $\alpha 1$  and one  $\alpha 2$  strands.<sup>[30]</sup> They are capped at the N- and C-termini by telopeptides, which have highly flexible structures<sup>[31,32]</sup> with only a few specific motifs. The N-terminal telopeptide forms a  $\beta I/II$  turn structure (D<sup>7</sup>EKS<sup>10</sup>), which is stabilized by a fairly strong hydrogen bond between

an aspartic acid (ASP<sup>7</sup>) and a serine (SER<sup>10</sup>).<sup>[29,28]</sup> At the C-terminus a sharp hairpin (PQPP)<sup>[30,33]</sup> is found in solution but the corresponding hydrogen network is not known.

Self-assembly of the natural triple helices is crucial for the formation and stability of fibrils, and telopeptides mediate the intermolecular interaction between collagen molecules.<sup>[34]</sup> The  $\alpha 1$  chains at both termini control the molecular recognition and the cross linking between two triple helices.<sup>[30,33]</sup> Inter- and intramolecular links at the N-terminus are important for linear fibril growth, whereas the C-terminus creates lateral intermolecular links.<sup>[35,36]</sup> During the formation of collagen fibrils the telopeptides interact with a receptor region of the triple helix partially unwinding its helical structure.<sup>[37]</sup> Adjacent molecules are linked by covalent bonds between lysine residues of the N-terminal telopeptide and lysine or hydroxylysine residues at the C-terminus of the triple helix region.<sup>[32,37]</sup> The present work contains a refined model of the collagen structure with full termination by telopeptides for reproducing the interaction of collagen triple helices with surfaces more realistically. We further take into account the influence of the intermolecular interaction of adjacent proteins on the surface reaction of a single molecule.

The description of the biointerface at an atomistic level is challenging because it combines both a complex protein structures and an oxide model, which must be extended beyond the perfect surface.<sup>[3,13,15]</sup> So far we investigated the adsorption of small collagen helix fragments<sup>[14]</sup> on hydroxylated flat rutile surfaces by classical molecular dynamics simulations.<sup>[12,17]</sup> In this study, we have defined a model of nanoscale structural elements on the stoichiometric (100) surface with two different degrees of roughness as suggested by STM experiments.<sup>[8,9]</sup> The chosen roughness of these models matches the length scales of the peptides considered here, and we present results of the tropocollagen and telopeptide interaction with the surfaces. In detail four topics are addressed:

- (i) analysis of the flexibility of collagen helices during classical molecular dynamic simulations
- (ii) helix–helix as well as helix–telopeptide interactions
- (iii) influence of the orientation of collagen with respect to the surface facets
- (iv) adsorption of one or more collagen–telopeptide systems on rough surfaces.

## Methods

The sequence of the telopeptides of rat tendon has been taken from Orgel *et al.*<sup>[30]</sup> Their structure file (1Y0F) in the Protein Data Bank (PDB)<sup>[38]</sup> refers to low resolution X-ray diffraction experiments (5.4 Å) and contains the positions of the C <sub>$\alpha$</sub>  atoms only of peptide chains with telopeptides and short triple helices. This was not appropriate for deducing a telopeptide terminated collagen model in atomistic detail. We instead generated two ideal triple helical conformations with the sequences from ref.<sup>[38]</sup> using the program triple helical collagen building script (THeBuScr<sup>[39]</sup>). The telopeptide

structures were obtained by reading the C<sub>α</sub> positions into xleap and obtaining a complete set of atomic positions for the residues from this program. The triple helices and the respective telopeptides were connected manually. The structure of the combined system was adapted to the data in ref.<sup>[38]</sup> by the following procedure: fixed mass points (pseudoatoms), representing the C<sub>α</sub> positions, were integrated into the model. By means of restrained molecular-dynamics simulations, the current C<sub>α</sub> atoms of the models were pulled to their experimental positions.<sup>[30]</sup> The two fragments were then subjected to molecular dynamics simulations for several ns and attained stable structures, where the telopeptide folds significantly deviated from the original X-ray data. The resulting fragments were combined resulting in a collagen triple helix which was fully terminated by telopeptides and had an overall length of about 130 Å.

Two rough rutile surfaces were generated (Fig. 1) both consisting of roof-like microfacets with (110) termination on a (100) base plane. The atomic charges of the slab oxygen and titanium atoms were -0.576 and 1.152 e, respectively.<sup>[40]</sup>

- (i) A (1 × 3) surface consists of facets on three elementary cells in [010] direction ( $a = 4.59 \text{ \AA}$ ) with widths and depths of 13.77 and 6.9 Å, respectively (Fig. 4 in ref.<sup>[8]</sup>). The facets have been integrated into the model for plane surfaces from ref.<sup>[17]</sup> by modifying three TiO<sub>2</sub> units (see Fig. 1).
- (ii) A more complex structure provides steps in [010] direction and lower and upper terraces containing two or three microfacets, respectively (Fig. 1, cf.<sup>[38]</sup>). The height of the steps is equal to the cell parameter  $a = 4.59 \text{ \AA}$ . The facets at the upper or lower level have widths of  $3a = 13.77 \text{ \AA}$ , whereas those including a step have widths of  $4a = 18.4 \text{ \AA}$ .

Hydroxylation equilibria for the aqueous titania surface have been calculated as on the perfect surface<sup>[17]</sup> derived from experimental data.<sup>[41]</sup> At pH = 7.4, 17% of the bridging oxygen atoms are protonated and 32% of the fivefold coordinated titanium atoms are hydroxylated, with charges of H<sup>+</sup> and OH<sup>-</sup> amounting to +1 and -1, respectively (cf.<sup>[12,17]</sup>). These formal charges represent an upper limit, but reproduce realistic adsorption energies for peptides.<sup>[12]</sup>

All systems were built using the xleap tool of the AMBER program package.<sup>[42]</sup> In cells containing titania, the slabs are aligned to the xy-plane. Atoms of the TiO<sub>2</sub> slabs were fixed in space, and the lengths of the bonds involving hydrogen were constrained by the SHAKE algorithm. Unless otherwise specified the full cell or the space between the surfaces, respectively, was filled with explicit TIP3P water molecules.<sup>[42]</sup> Na<sup>+</sup> and Cl<sup>-</sup> ions neutralized the charged surface

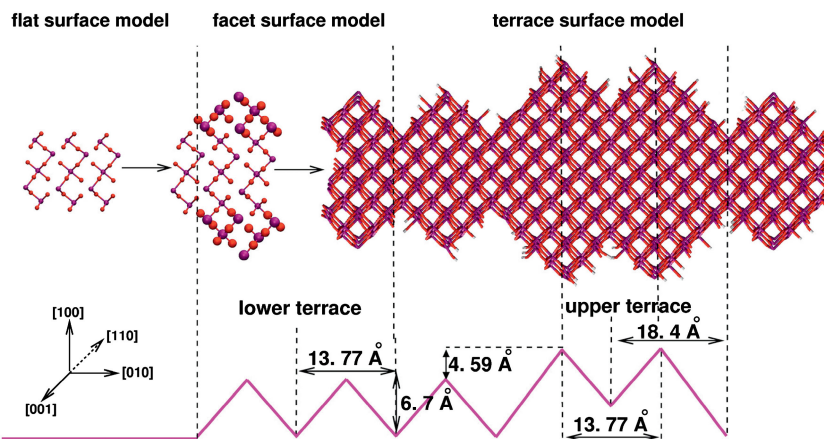


Fig. 1. Two models of rough surfaces derived from the flat surface model (left), which has been assembled from TiO<sub>2</sub> units repeating them in *x* and *y* direction.<sup>[12,17]</sup> Oxygen and titanium atoms are colored red and magenta: (1) microfacets have been generated by prolonging the TiO<sub>2</sub> units as indicated by bold spheres, (2) steps with a height of one TiO<sub>2</sub> layer have been introduced resulting in a terrace structure.

and reproduced the physiological ionic concentration of 0.15 mol·L<sup>-1</sup> in the bulk. Periodic boundary conditions in all systems resulted in stable water structures and contiguous rutile surfaces.

Two types of cells contained proteins in aqueous solution only for studying the properties of single molecules and their mutual interaction:

- (i) Long fragments of the pure helical regions (300 Å) in cells with a size of 322 × 43 × 35 Å<sup>3</sup> and about 15 000 water molecules were used for reproducing the Young's modulus of collagen helices. The sequence was taken from ref.<sup>[30]</sup> Two peptides 10.2 Å above a plane (100) surface did not show stable adsorption, since the mutual interaction was strong. This system was analyzed in terms of peptide-peptide interaction only.
- (ii) A second set of systems consisted of one or two collagen triple helices fully capped with telopeptides in simulation cells with sizes up to 183 × 82 × 137 Å<sup>3</sup> filled by up to 63 000 water at standard density. These collagen models with lengths of 130 Å were used for simulating helix-helix as well as helix-telopeptide interactions.

The influence of surface roughness on the adsorption of the peptides was analyzed building various sequences of facets and steps on rutile (100) systems and positioning collagen fragments in parallel to the surface:

- (iii) A number of initial configurations provided a short uncapped 80 Å collagen fragment<sup>[14]</sup> oriented perpendicularly or parallel with respect to the grooves in cells with cross sections of up to 156 × 45 or 79 × 100 Å<sup>2</sup>, respectively. The two protein orientations were parallel to [010] (Fig. 2A, top) and [001] (Fig. 2A, bottom) directions, respectively (cf. Fig. 1). The cells had total heights around 90–95 Å and spacings of about 70–75 Å in *z*-direction between titania slabs and their images, being filled with about 9000–20 000 water molecules.

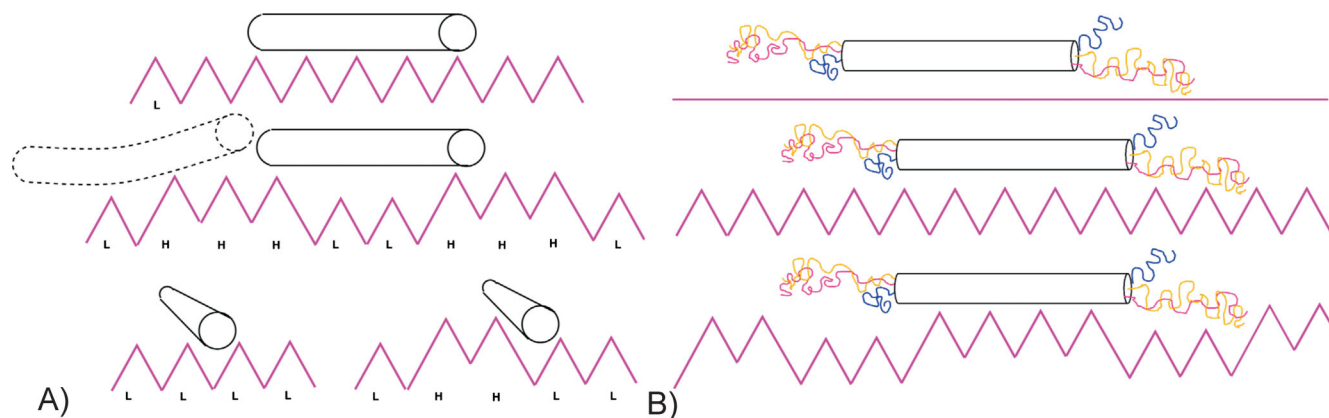


Fig. 2. (A) schematic view of initial configurations of small collagen fragments on rough surface structures. The indices (L) and (H) denote the sequence of lower and higher microfacets, respectively. From top to bottom: (1) collagen along [010] direction on a microfaceted surface, (2) collagen along [010] direction on terrace surface model with different initial positions on two upper terraces (solid line) and on a step (dashed line) (3) collagen molecule along [001] direction on a faceted surface model and at a step on the terrace structure model. (B) Schematic view of the fully terminated collagen on (from top to bottom) a flat surface, a microfaceted surface and a surface with terrace structure; all molecules have initial orientations along [010] direction.

(iv) A further set of systems contained one or two collagen molecules with lengths of 130 Å fully terminated by telopeptides, in initial configurations vertical to the grooves ([010], Fig. 2B) of the rough surfaces. The surfaces had to be extended to dimensions of up to 193 × 71 Å<sup>2</sup>. The cells were as high as 140 Å for minimizing the interaction of the proteins with the image surface in z-direction. After filling the vacuum with up to 46 000 water molecules, helix–surface interactions were simulated in competition with helix–telopeptide interactions. As results from the 80 Å fragments [systems (3)] had suggested that stronger adhesion was seen on [010] than on [001] direction, the latter one was omitted for these huge cells.

For all simulations the sander program in the AMBER10 suite was employed.<sup>[42]</sup> Atomic images were generated and the secondary structures of the peptides were analyzed in VMD.<sup>[43]</sup> Standard procedures of filling the simulation cell with water solvent result in incomplete packing with densities around 0.8 g·cm<sup>-3</sup>. Optimum solvent density is attained by reducing the cells size, usually by adjusting the *x*, *y*, and *z* dimensions of the box during an NpT run (constant particle number *N*, pressure *p*, and temperature *T*). In cells with a titania slab, this procedure would disrupt the contiguous oxide surface, and only the cell height *z* is reduced in steps of 0.1 Å without displacing the water molecules. Overlap between those close to the top of the cell and to the bottom of its mirror image is cured by short intermediate energy minimization and molecular dynamics runs at constant volume and a controlled temperature of 500 K (NVT) with fixed protein.<sup>[12,17]</sup> After cell size adjustment, energy minimization was done in three steps: first only the water molecules were relaxed, and the protein was fixed, then the protein was relaxed inside the fixed water box, and finally the energy of the whole system was minimized. The minimized

systems were subjected to relaxation runs at 300 K for 0.5 ns (NVT). Production runs in the range of 10–22 ns for tracing the dynamics of the proteins on the surface as well as the formation of contact points have been performed without temperature control (NVE). Under these conditions the stability of the system could be appreciated and processes with dissipation of significant amounts of potential energy could be detected by a temperature rise. The time step for molecular dynamics was 1 fs.

The 300 nm collagen strand was subjected to mechanical stress by harmonic restraints on the distance between both ends with force constants in the range 0.12–0.3 N·m<sup>-1</sup>. The set point was extended continuously with rates of 1–4 m·s<sup>-1</sup>. The effective force was evaluated by Hooke's law from the difference between set point and actual value of the restrained distance.<sup>[12]</sup> Restrained molecular dynamics simulations were performed in vacuum, in implicit water environment and with explicit TIP3P water molecules for checking the influence of the environment on the calculated mechanical stiffness of the molecule. The nominal stress  $\sigma$  is calculated from these data as force divided by area of the collagen triple helix with a mean diameter of 15.7 Å,<sup>[29]</sup> and the strain  $\epsilon$  is the change in length ( $L-L_0$ ) divided by the original length  $L_0=300$  Å (Fig. 3A).

## Results and Discussion

### Flexibility of Collagen Strands

Restrained molecular dynamics simulations were performed for validating our collagen model by comparing its mechanical properties with experimental data. Experiments on entropy driven elastic forces of a few pN,<sup>[25]</sup> corresponding to stress of about 5 MPa, could not be reproduced by our force field simulations. Such restoring forces are lower than the noise due to thermal motion. We applied forces up to 8 nN and assigned the resulting strain to stretching mechanisms

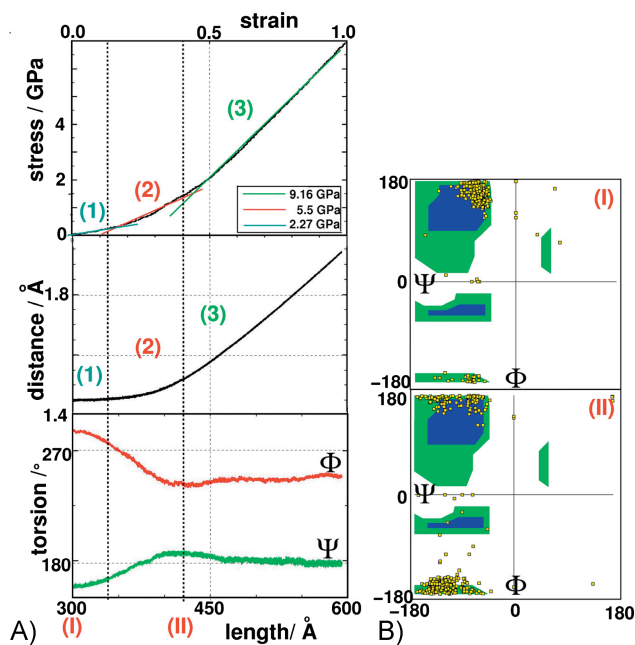


Fig. 3. (A) History of stress (top), of the mean C–C bond length (middle) and of torsion angles  $\Psi$ ,  $\Phi$  (bottom) in the peptide backbone of a 300 Å collagen triple helix fragment in explicit water environment. The stretching rate was  $4 \text{ m}\cdot\text{s}^{-1}$  with a force constant of  $0.3 \text{ N}\cdot\text{m}^{-1}$ . (1) In the first range of mechanical stress on the helix the molecule is forced into a fully linear structure. Bond lengths and torsions remain nearly unchanged. (2) In the second range (340–420 Å) the torsion angles shift from triple helical configuration to ( $\Phi$ ,  $\Psi$ ) values of (180, 240°). (3) Stretching the molecule to more than 420 Å, results in increased bond lengths, as the torsion angles have already reached the maximal stretched conformation. (B) (top) Ramachandran plot of the relaxed collagen fragment,  $\Psi$  and  $\Phi$  values representing the typical triple helix area of collagen, (bottom) stretching the molecule to a length of 420 Å shows a shift of torsion angle  $\Psi$  and  $\Phi$  from triple helical configuration toward a  $\beta$  sheet like configuration.

(Fig. 3A). Coinciding force distance relations have been obtained for a variety of restraint force constants, expansion rates and environments.

- (i) Between  $L = 300$  and  $340 \text{ Å}$ , at a strain below 0.13, the length of the triple helix increased without significant structural changes. The backbone torsional angles were still in the typical ranges for collagen (Fig. 3B, top), and bonds lengths and angles were close to their equilibrium values (Fig. 3A). The restoring force corresponded to a Young's modulus of about 2 GPa, which is comparable to experimental values between 3 and 5 GPa at low strains.<sup>[27,28]</sup>
- (ii) Between 340 and  $420 \text{ Å}$ , up to a strain of 0.4, torsions, which show the weakest resistance to external stress among all bonded interactions, relaxed (Fig. 3A, bottom), and the backbone dihedrals ( $\Phi$ ,  $\Psi$ ) shifted from values around (285°, 160°) (Fig. 3B, top) toward (245, 185°) (Fig. 3B, bottom). The helices started to untwist and attained linearly stretched structures. The corresponding Young's modulus was about 5 GPa.
- (iii) Around  $420 \text{ Å}$ , the torsions had already relaxed into the maximally extended conformation (Fig. 3A, bottom), and further external stress directly affected bond lengths and angles (cf. ref.<sup>[24,25]</sup>). These are described by harmonic

potentials, and the extension of the molecule still followed Hook's law corresponding to a Young's modulus as high as 10 GPa.

#### Interaction Between Two Strands (Helix–Helix Interaction)

Calculations scanning real times up to 22 ns, with two long (300 Å) independent collagen fragments in one cell, revealed that the mutual interaction of adjacent helices mainly consisted of hydrogen bonds between the side chains of the residues located in the two C- and N-terminus regions, respectively. Initially, the helices had a closest atom-atom distance of about 15 Å. The first very weak contact between a lysine side chain in the C-terminus and a hydroxyproline residue in the other one with an H(LYS)–O(HYP) distance of 3.5 Å was observed after 1.2 ns. The helices were slightly displaced with respect to each other and after 3.5 ns a first stable hydrogen bond between a glutamic acid and a lysine side chain was established. The number of hydrogen bonds increased during the simulation. After 10 ns five additional stable hydrogen bonds with (N)H–O distances in the range of 1.8–3.0 Å were formed at the N-terminus, mostly involving proline or hydroxyproline. During the whole simulation time about ten hydrogen bonds were detected mainly involving reactive charged amino acids like aspartic acid.

#### Telopeptides

Only few specific conserved secondary structure motifs in telopeptides (Fig. 4A) are known from experiments,<sup>[31,32]</sup> especially two types of  $\beta$ -turns, the  $\beta$ I/ $\beta$ II (DEKS) turn and the hairpin (PQPP) structure in the  $\alpha$ 1 N-terminus<sup>[32]</sup> and C-terminal telopeptide strands,<sup>[30,33]</sup> respectively. According to ref.<sup>[32]</sup> the  $\beta$ -turns are essential for the intermolecular interaction of telopeptide regions with the collagen helices.

The torsion angles  $\psi_i + 1$  and  $\phi_i + 1$  describe the GLU<sup>8,156</sup> position in the  $\beta$  DE<sup>8,156</sup>KS turns and the GLN<sup>75,223</sup> position in the (PQ<sup>75,223</sup>PP) hairpin structure of the  $\alpha$ 1 chains, and  $\psi_i + 2$  and  $\phi_i + 2$  refer to LYS<sup>9,157</sup> resp. PRO<sup>76,224</sup>.<sup>[31]</sup> The distribution of simulated torsion angles (Fig. 4B) of one  $\alpha$ 1 chain,  $\alpha$ 1a in Figure 4A, is in good agreement with the angles proposed for a  $\beta$ I (DEKS) turn in ref.<sup>[31]</sup> The structure was stabilized by a hydrogen bond between ASP<sup>7</sup> and SER<sup>10</sup>, which was closed during the simulation time independently of the number of molecules in the cell or their surface contact. The N-terminal  $\beta$ I (DEKS) turn motif was only found in the  $\alpha$ 1a chain, not in both  $\alpha$ 1 ends, as proposed in ref.<sup>[31]</sup>. The structure of the second chain ( $\alpha$ 1b in Fig. 4A), corresponds to none of the turns  $\beta$ I or  $\beta$ II (Fig. 4B). We attribute this discrepancy to a stable hydrogen bond between GLU<sup>156</sup> and SER<sup>158</sup> in  $\alpha$ 1b rather than between ASP<sup>155</sup> and SER<sup>158</sup> in  $\alpha$ 1a leading to a distribution of torsion angles different from the  $\beta$ I (DEKS) turn. The lifetimes of these two hydrogen bonds to SER were two to three times higher than those in the remaining telopeptide structure indicating a high stability of the  $\beta$  turn regions. The C-terminal hairpin (PQPP) in our model has been specified as a  $\beta$ VIB turn

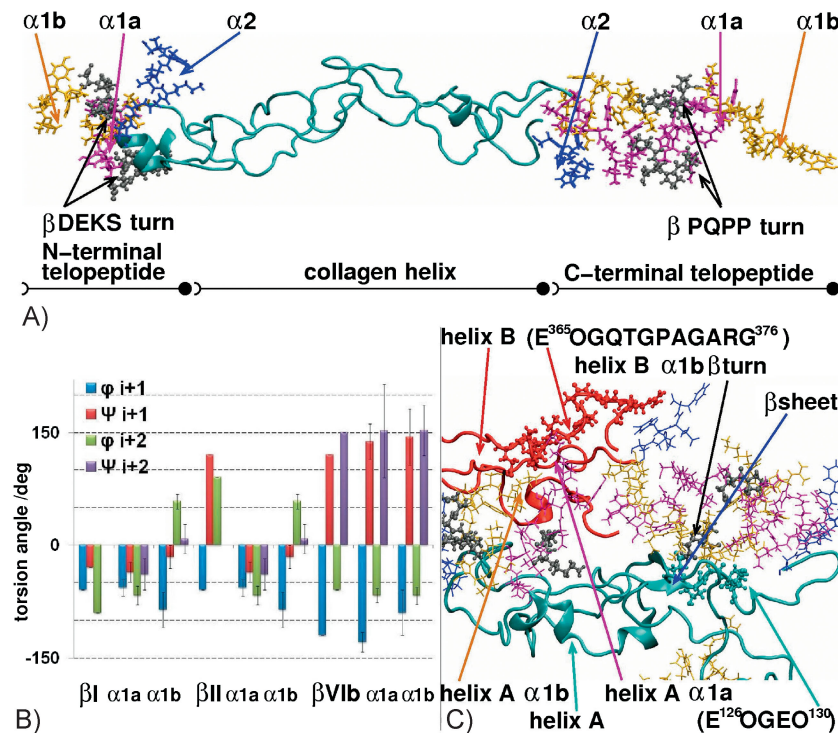


Fig. 4. (A) fully terminated collagen molecule model, coloring scheme: (magenta) N- and C-terminal telopeptide  $\alpha 1a$  chain, (orange)  $\alpha 1b$  chain, (blue)  $\alpha 2$  chain, (cyan) collagen triple helical region, (black) N- and C-terminal  $\beta$  turn motives. (B) Bar chart of torsion angles  $\varphi$  and  $\Psi$  averaged over the simulation time with standard deviation (black lines) in the  $\beta$  turn motives of N- and C-terminal telopeptides: (from left to right)  $\beta I$  (DEKS) turn from ref.<sup>[31]</sup> DEKS motives in modeled chains  $\alpha 1a$  and  $\alpha 1b$ ,  $\beta II$  (DEKS) turn from ref.<sup>[31]</sup> DEKS motives in modeled chains  $\alpha 1a$  and  $\alpha 1b$ ,  $\beta VIb$  (PQPP) turn from ref.<sup>[31]</sup>, PQPP motives modeled in chains  $\alpha 1a$  and  $\alpha 1b$ . The conformations of DEKS in  $\alpha 1a$  and of PQPP in both  $\alpha 1$  chains coincide with  $\beta I$  and  $\beta VIb$ , respectively. (C) Interplay of telopeptides and helical receptor region: N-terminal telopeptide of molecule A interacts with helical  $\alpha 2$  chain, C-terminal telopeptide ( $\beta VIb$  turn of chain  $\alpha 1b$ ) of molecule B builds a connection complex with helix A.

(Fig. 4B) in good agreement with<sup>[44]</sup> postulating stabilization by a cis-peptide bond with proline rather than by H-bonds.

The two  $\alpha 1$  strands in one collagen molecule were interconnected by several short lived hydrogen bonds. The most stable ones linked the ends of the  $\alpha 1a$  and  $\alpha 1b$  chain (Fig. 4A) closing and opening in intervals of 1–4 ns over the simulation time of about 15 ns. The central part of the telopeptides showed no specific hydrogen network and maintained great flexibility. Our torsion angles of both  $\alpha 1$  chains are in good agreement with the measured values of a hairpin structure<sup>[30,33]</sup> (Fig. 4B). The shorter  $\alpha 2$  chain had no hydrogen bond interactions with the  $\alpha 1$  chains and had random structure over the modeled systems.

#### Interaction Between Two Strands (Helix–Telopeptide Interaction)

From investigations of the telopeptide–helix interaction an atomistic picture of the link between the (PQPP) turn and a receptor region in the triple helix arose. The simulation of two collagen helices terminated with telopeptides resulted in a hydrogen bond between glutamic acid (GLU<sup>1</sup>) of the  $\alpha 1a$  chain of the N-terminal telopeptide of molecule A and the hydroxyproline (HYP<sup>366</sup>) in the helical region of the  $\alpha 2$  chain of molecule B (Fig. 4C). A second hydrogen bond connected

serine (SER<sup>151</sup>) of the  $\alpha 1b$  chain and the helical glutamic acid (GLU<sup>365</sup>). Both amino acids of the  $\alpha 1$  chains are not part of the  $\beta$  (DEKS) motifs, and the  $\beta$ -turns of the N-terminal telopeptide have never been involved in the intermolecular interaction even though their lysine residues had been considered as cross linker in ref.<sup>[30,32,37]</sup>.

During the last ns of the simulation time, another short lived hydrogen bond between a phenylalanine (PHE<sup>384</sup>) of the C-terminal telopeptide  $\alpha 2$  chain of helix A and an arginine (ARG<sup>375</sup>) in the receptor region of helix B was established. The binding of the telopeptide to the helical region ( $E^{129}OGQTGPAGARG^{140}$ ) induced local conformational changes of the amino acids between HYP<sup>125</sup> and GLY<sup>129</sup> next to the contact. Here, the opening of the helix and formation of a sort of a bubble was observed. The analysis of the torsion angles revealed a shift from the  $\alpha$ - into the  $\beta$ -sheet range. It could be speculated that the formation of such contacts to telopeptides might only be possible for specific helix sequences, and that this might induce an ordered assembly of triple helices. At the same time the C-terminal  $\alpha 1b$  telopeptide chain of helix B interacts with the  $\alpha 2$  helical chain of helix A ( $E^{126}OGEO^{130}$ ). In this case the hydrogen bond was formed between the helical and GLU<sup>126</sup>/HYP<sup>127</sup> and GLN<sup>459</sup> on the  $\beta VIb$  turn.

#### Adsorption of the Uncapped 80 Å Fragment on the Rough TiO<sub>2</sub> Surfaces

In one run, the peptide was oriented in [001] direction on top of a microfacet (Fig. 2A bottom) and had one initial contact between the amino group of a lysine and a singly coordinated surface hydroxyl group at the edge of a facet. This contact was stable during the whole simulation time with an average N–O distance around 2.7 Å. The diameter of 15.7 Å of the collagen triple helix was too big for insertion into a groove with a depth of 6.7 Å, and the collagen could only be adsorbed on top of the facets. Amino acids with short side chains could not reach the sides of the facets, but long side chains could easily penetrate into the valley between the microfacets with top to top distances of 13.77 Å. One N-terminal group attached to the opposite side of the roof with a constant average N–O distance of 2.2 Å. The helix bent away from the surface and attained a tilted structure. The formation of localized contacts between a still flexible helix and the flat surface was also observed in ref.<sup>[14]</sup>

The protein on a step of the terrace structure ([001] orientation), rolled over the top of the edges toward the lower terrace after 1.5 ns. Contacts between amino acids and the

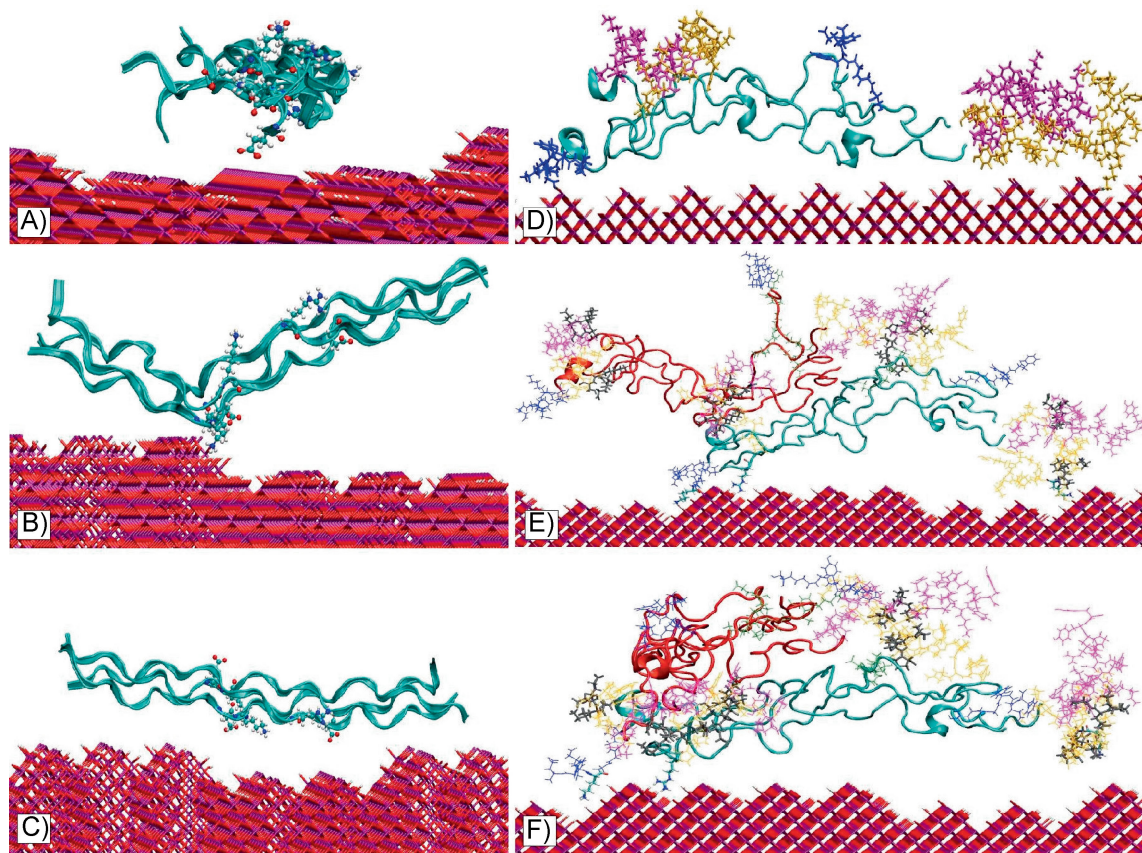


Fig. 5. Uncapped (A–C) and capped (D–F) triple helices on the terrace surface drawn as ribbons. In (A–C) the charged side chains are plotted as balls and sticks for indicating their sizes with respect to surface roughness. In (E–F) explicit structures of the telopeptides are shown demonstrating their surface interaction. (A) Initially the 80 Å fragment is weakly adsorbed on top of the microfacets and rolled along its axis to the lower terrace, (B) stable adsorption on the step via a single lysine side chain with an average N–O distance of 2.7 Å, the helix remaining flexible, (C) perpendicular orientation with respect to the grooves, the ends of the helix lie on two upper terraces and the reactive side chains face the lower terrace. The molecule did not bend into the valley, but moved along [010] direction and attained an adsorbed configuration similar to (B). (D) Adsorption of the fully terminated telopeptide was stable on a faceted model surface, the telopeptides entering the grooves, (E) initial configuration of two capped collagen molecules on a terrace surface model, (F) system (E) after 10 ns of molecular dynamics simulation. The C-terminal telopeptide of the upper molecule attached to the helical receptor region of the bottom molecule, and initiated the desorption of its C-terminus.

surface of the step were weak with O–H and N–O distances around 5 Å between negatively charged amino acids like aspartic and glutamic acid or positive lysine and oppositely charged singly and doubly coordinated hydroxyl groups, respectively (Fig. 5A).

In [010] orientation perpendicular to the grooves, on the purely (1 × 3) microfaceted model (Fig. 2A top), the protein attached to the surface via several charged nitrogen containing groups. A stable link between an arginine side chain and the edge of a hydroxylated facet had an average N–O distance of 2.5 Å. Two lysine side chains interacted with various singly coordinated hydroxyl groups during the whole simulation time with average N–O distances of 2.7 Å. Similar fluctuating lysine contacts had been observed on hydroxylated flat rutile (100) surfaces.<sup>[14]</sup> Another contact was formed between an N-terminal amino group and the lower edge of a microfacet. Aspartic or glutamic acid side chains are shorter than those in lysine and arginine, and as a consequence they could not attach to the grooves.

In further runs, helices have been oriented perpendicular to the grooves of the terraced surface ([010] orientation,

cf. Fig. 2A, middle, left). An initial lysine contact of the helix positioned close to only one step was stable during the simulation time of 6.5 ns (Fig. 5B). A further link between the amino part of an asparagine carbon amid group and a singly coordinated hydroxyl group was formed after less than one ps. The helix was attached to the surface only by these two contacts with average N–O distances of 2.7 Å. The molecule was still flexible and slightly bent (cf. ref.<sup>[14]</sup>), forming no links to the lower terrace. No more than every third to fourth GXP triplet contains a charged residue<sup>[45]</sup> (cf. Fig. 5B), and only these regions have attractive interactions to the strongly hydrophilic titania surface.

In a terrace system with the helix oriented along [010] direction (Fig. 2A middle, right), the two ends of the fragment contacted the two upper terraces, bridging the two microfacets on lower terrace. The charged amino acids, which generated the surface contact in the other systems, were located above the lower terrace (Fig. 5C). The fragment did not bend for approaching these side chains to the surface, but moved along [010] direction by about 20 Å within 3.5 ns and was immobilized at a final position with lysine contacts on a step

for another 5.5 ns. The triple helix could not adapt to the lower terraces by bending, and reactive side chains were not able to reach even the top of the facets.

#### *Tropocollagen on the Rough TiO<sub>2</sub> Surfaces*

The telopeptides are significantly more flexible than the triple helical regions, and adsorption of fully terminated collagen molecules on the faceted surface is less hindered by roughness than that of the uncapped fragments discussed so far (Fig. 5D).

On the terrace structure the helical part of the fragment again was not able to adapt to the roughness, since the length scale of the roughness in the (1 × 3) microfacet model is smaller than the typical curvature radius of a telopeptide chain. The helical region was lying on top of an upper terrace maintaining its flexibility, and only arginine and lysine residues in the α1 chains of the telopeptide formed surface contacts. As our force field has reproduced the mechanical properties of collagen in very good agreement with experimental data, we assume that the stiffness of the helix is not an artifact of the model parameters but that steric hindrance of adsorption on rough surfaces may be expected.

The situation was more complex with two fully terminated collagen molecules in the system. One molecule had an initial configuration close to the surface (Fig. 5E, cyan helix), and the second one was lying on top of it (Fig. 5E red helix). The β (P<sup>458</sup>QPP<sup>461</sup>) turn in the C-terminal telopeptide of this second collagen was attached to the helix of the adsorbed molecule pulling its C-terminus away from the surface (Fig. 5F), whereas surface adsorption of arginine and lysine side chains at the N-terminus was not affected.

#### *Conclusions*

Only thanks to the DEISA supercomputing resources it was possible to observe helix–helix interactions in this very large system by atomistic molecular dynamics simulations over times long enough to trace fibril flexibility and we observed the beginning of the association into fibrils. Significant longer time scales are necessary to reproduce the whole dynamics, and cross-linking was so far only studied by means of coarse grain models.<sup>[46]</sup>

In a realistic system, peptides in solution will first undergo full relaxation and concentration dependent association before reaching the surface. This procedure is out of reach of the atomistic simulations, so far, and a large number of initial configurations have to be run instead for reducing the influence of the conditions on the results.

Calculations with two different surface structures derived from the experiment demonstrate the crucial importance of the flexible telopeptides during adsorption processes. In our purely (1 × 3) faceted model surface roughness had only minor influence on the adsorption of the helical structure or the telopeptide. On the terrace model the triple helices are too rigid for stable adsorption, but the flexible telopeptides adsorbed even at the lower terraces and were not influenced

by roughness. The large system might have a more continuum like behavior than the small fragments.

The interplay of telopeptide and helix as well as the surface reactions have been investigated stepwise and an atomistic picture of driving forces for the self-assembling to collagen fibrils has emerged. The competition between protein–protein interaction and adsorption to the surface was clearly observed. The building of collagen fibrils from five triple helices could be entropy driven similar to some steps of protein folding,<sup>[47]</sup> whereas surface adsorption of the molecule is enthalpy driven and reduces the entropy of the flexible adsorbates. The role of entropy probably increases with increasing helix lengths and curvatures. The role of helix–telopeptide interaction in the mechanism of collagen fibrillogenesis is not yet assessed. Experimental data show a periodicity of 670 Å in collagen fibrils<sup>[47]</sup> and we speculate that this may be assisted by flexible end groups of natural tropocollagen such as telopeptides.

*Received: October 15, 2010*

*Final Version: April 6, 2011*

*Published online: June 1, 2011*

- [1] S. Teng, E. Lee, C. Park, W. Choi, D. Shin, H. Kim, *J. Mater. Sci.: Mater. Med.* **2008**, *20*, 2553.
- [2] H. Schliephake, A. Aref, D. Scharnweber, S. Bierbaum, A. Sewing, *Clin. Oral Impl. Res.* **2009**, *21*, 31.
- [3] H. Chen, X. Su, K. Neoh, W. Choe, *Langmuir* **2008**, *24*, 6852.
- [4] M. E. Nagassa, A. E. Daw, W. G. Rowe, A. Carley, D. W. Thomas, R. Moseley, *Clin. Oral Impl. Res.* **2008**, *19*, 1317.
- [5] W. Song, H. Chen, *Chin. Sci. Bull.* **2007**, *52*, 3169.
- [6] Y. F. Dufrene, T. G. Marchal, P. G. Rouxhet, *Langmuir* **1999**, *15*, 2871.
- [7] G. J. Szöllösi, I. Derenyi, J. Vörös, *Physica A* **2004**, *343*, 359.
- [8] P. W. Murray, F. M. Leibsle, C. A. Muryn, H. J. Fisher, C. F. J. Flipse, G. Thornton, *Phys. Rev. Lett.* **1994**, *72*, 689.
- [9] P. W. Murray, F. M. Leibsle, H. J. Fisher, C. F. J. Flipse, C. A. Muryn, G. Thornton, *Phys. Rev. B* **1992**, *46*, 12877.
- [10] V. Caravetta, S. Monti, *J. Phys. Chem. B* **2006**, *110*, 6160.
- [11] S. Köppen, O. Bronkalla, W. Langel, *J. Phys. Chem. C* **2008**, *123*, 14600.
- [12] S. Köppen, W. Langel, *Langmuir* **2010**, *26*, 15248.
- [13] A. A. Skelton, T. Liang, T. R. Walsh, *Appl. Mater. Interfaces* **2009**, *1*, 1482.
- [14] S. Köppen, B. Ohler, W. Langel, *Z. Phys. Chem.* **2007**, *231*, 3.
- [15] S. Monti, *J. Phys. Chem. C* **2007**, *111*, 6086.
- [16] M. Chen, C. Wu, D. Song, K. Li, *Phys. Chem. Chem. Phys.* **2010**, *12*, 406.
- [17] S. Köppen, W. Langel, *Surf. Sci.* **2006**, *600*, 2150.



- [18] I. Streeter, N. H. de Leeuw, *J. Phys. Chem. B* **2010**, *114*, 13263.
- [19] S. Monti, S. Bronco, C. Cappelli, *J. Phys. Chem. B* **2005**, *109*, 11389.
- [20] T. Hayashi, K. Sano, K. Shiba, K. Iwahori, I. Yamashita, M. Hara, *Langmuir* **2009**, *25*, 10901.
- [21] M. Chen, C. Wu, D. Song, W. Dong, K. J. Li, *Mater. Sci. : Mater. Med.* **2009**, *20*, 1831.
- [22] H. S. Gupta, in: "Structure and Mechanics of Collagen Type I Tissues in Vertebrates" (Ed: P. Fratzl), Springer-Verlag, New York **2008**, pp. 155–173.
- [23] Y. L. Sun, Z.-P. Luo, A. Fertala, K. N. An *Biochem. Biophys. Res. Commun.* **2002**, *295*, 382.
- [24] M. J. Buehler, *PNAS* **2006**, *103*, 12285.
- [25] M. J. Buehler, *J. Mater. Res.* **2006**, *21*, 1947.
- [26] A. Gautieri, S. Vesentini, F. M. Montevercchi, A. Redaelli, *J. Biomech.* **2008**, *41*, 3073.
- [27] H. Hofmann, T. Voss, K. Kühn, *J. Mol. Biol.* **1984**, *172*, 325.
- [28] N. Sasaki, S. Odajima, *J. Biomech.* **1996**, *29*, 655.
- [29] S. Vesentini, C. F. C. Fitie, F. M. Montevercchi, A. Redaelli, *Biomech. Model. Mechanobiol.* **2005**, *3*, 224.
- [30] J. P. Orgel, T. J. Wess, A. Miller, *Structure* **2000**, *8*, 137.
- [31] A. Otter, G. Kotovych, P. G. Scott, *Biochemistry* **1989**, *28*, 8003.
- [32] J. P. Malone, A. George, A. Veis, *Proteins* **2004**, *54*, 206.
- [33] M. Buckley, M. Collins, J. Thomas-Oates, *Anal. Biochem.* **2008**, *374*, 325.
- [34] T. J. Wess, A. P. Hammersley, L. Wess, A. Miller, *J. Mol. Biol.* **1998**, *275*, 255.
- [35] J. P. R. O. Orgel, T. C. Irving, A. Miller, T. J. Wess, *PNAS* **2006**, *103*, 9001.
- [36] P. X. Qi, E. M. Brown, *JALCA* **2002**, *97*, 235.
- [37] J. P. Malone, A. Veis, *Biochemistry* **2004**, *43*, 15358.
- [38] www.pdb.org.
- [39] J. K. Rainey, M. C. Goh, "Bioinformatics", Oxford University Press, **2004**, page 1.
- [40] V. Swamy, J. D. Gale, *Phys. Rev. B* **2000**, *62*, 5406.
- [41] C. E. Giacomelli, M. J. Avena, C. P. DePauli, *Langmuir* **1995**, *11*, 3483.
- [42] W. D. Cornell, P. Cieplak, C. I. Bayly, I. R. Gould, K. M. Merz, Jr, D. M. Ferguson, D. C. Spellmeyer, T. Fox, J. W. Caldwell, P. A. Kollmann, *J. Am. Chem. Soc.* **1995**, *117*, 5189.
- [43] W. Humphrey, A. Dalke, K. Schulten, *J. Mol. Graphics* **1996**, *14.1*, 33.
- [44] J. S. Richardson, *Adv. Protein Chem.* **1981**, *34*, 167.
- [45] J. Bella, M. Eaton, B. Brodsky, H. M. Berman, *Science* **1994**, *266*, 75.
- [46] M. Buehler, *J. Mech. Behav. Biomed. Mater.* **2008**, *1*, 59.
- [47] D. J. Voet, J. G. Voet, C. W. Pratt, in: *Biochemistry*, 3rd Edn. John Wiley & Sons, Asia, **2008**, p. 162.